Desalination and Water Treatment
www.deswater.com

doi: 10.5004/dwt.2020.26384

205 (2020) 264–274
November

Employing UV/periodate process for degradation of p-chloronitrobenzene in aqueous environment

Aref Shokri[a,*], Hojatollah Moradi[b], Majid Abdouss[c], Bahram Nasernejad[d]

[a]*Department of Chemistry, Faculty of Science, Payamenoor University, Tehran, Iran, email: aref.shokri3@gmail.com (A. Shokri)*
[b]*Surface Phenomenon and Liquid–Liquid Extraction Research Lab, School of Chemical Engineering, University College of Engineering, University of Tehran, Tehran, Iran*
[c]*Department of Chemistry, Amirkabir University of Technology, Tehran, Iran*
[d]*Department of Chemical Engineering, Amirkabir University of Technology, Tehran, Iran*

Received 26 February 2020; Accepted 25 July 2020

ABSTRACT

In this study, the potassium periodate was activated by ultraviolet (UV) light in UV/KPI process, and it was used for degradation of p-chloronitrobenzene (pCNB) in an aqueous environment. The full factorial design (FFD) and artificial neural networks (ANN) were used to investigate the influence of experimental parameters including temperature (*T*), initial concentration of periodate ([KPI]), and pH on the removal of pCNB. The optimum conditions in the treatment of 50 mg/L of the pCNB were achieved at 300 mg/L of KPI, pH of 7, and Temperature at 35°C. At optimum condition, the removal of pCNB was 97.8% (experimental), and the predicted amount by ANN and FFD were 97.79% and 99.02%, respectively. The chemical oxygen demand removal percent was 64.3% after 90 min of reaction. Although, the ANN was better than FFD model, and the root mean square error of ANN was lower than FFD model ($1.0268_{AAN} < 2.055838_{FFD}$). The ANN needs larger sets of data and computational time. A high correlation coefficient ($R^2_{ANN} = 0.9974$, $R^2_{FFD} = 0.9886$) was achieved by an evaluation between the results of the model and experimental. The average percentage error for FFD and ANN were 1.570615 and 0.4328, respectively, signifying the advantage of ANN in taking the nonlinear presentation of the system.

Keywords: p-chloronitrobenzene (pCNB); UV-activated potassium periodate (UV/KPI); Full factorial experimental design (FFD); Artificial neural network (ANN)

1. Introduction

Given the limited amount of fresh water supplies, human life is in danger at current decades, so the treatment and reuse of water is a very important anxiety [1]. The pCNB is a classic halogenated nitro aromatic contaminant that is mostly used in the manufacture of pesticides, herbicides, antioxidants, and other industrial chemicals. It can hold mutagenic and carcinogenic properties and cause methemoglobinemia in human and animals. So, the removal of pCNB in aqueous solution is important for human health and environment [2]. Degradation of pCNB is very difficult and requires long treatment time based on the powerful electron withdrawing features of nitro group affecting the pCNB molecules to be more stable.

The typical approaches in remediation of wastewater comprises different procedures; the contaminant was only transferred from one phase to another by most of them and a new and another type of pollution are come across and additional treatments are required [3]. Therefore, the advanced oxidation processes (AOPs) are self-reliant in degradation and mineralization of contaminants in aqueous environments and converting them to water, carbon dioxide, and other mineral oxides in aqueous solutions. The AOPs can generate hydroxyl radical that is the second strongest famous oxidant after fluorine.

* Corresponding author.

Large number branches of AOPs can degrade the pollutants to harmless inorganic compounds without secondary pollution [4,5].

The potassium periodate activated by UV (UV/KPI process), is one of the main branch of AOPs that is developed recently. The active species such as $IO_4^{\bullet}$, $OH^{\bullet}$, and $IO_3^{\bullet}$ have been formed from UV/KPI process which can oxidize the organic contaminants in the aqueous phase rapidly [6]. The photo-activation of periodate ions can accelerate the production of high reactive hydroxyl radicals [7]. At first, the periodate ion is decomposed by photo to produce $O^{\bullet-}$ and $IO_3^{\bullet}$ species via the transmission of one electron, and an acidic proton was adsorbed by anion radical oxygen, $O^{\bullet-}$ and the hydroxyl radical was produced. Also, periodate ions may change to $H_4IO_6^-$ ion molecule by reacting with two water molecules and generating hydroxyl radicals [8]. Furthermore, it has been reported that the iodine compounds can be recovered by ionic exchange and they can be regenerated electrochemically to produce periodate species [9].

Recently, much attention paid to full factorial experimental design (FFD) and artificial neural networks (ANN) because they have been employed effectively as an optimization and modeling tools to solve complicated and highly nonlinear problems [10,11]. As a result, FFD and ANN relate to modeling approaches that dealing with the progress of non-parametric simulative models. Actually, these models by real observed data calculate the real relations between independent (input) and dependent variables (response). Also, the models are used to estimate the optimum set of independent variables to minimize or maximize the response of dependent variables [12,13]. The FFD is one of the multivariate methods that can deal with statistical modeling and experimental design. It is used to inspect the correlation between one or more response variables and a set of numerical experimental factors or variables. The ANN modeling, which was motivated from the working of biological nervous organisms, has demonstrated to be an influential method for complex and nonlinear problems with strong capability to learn and forecast.

But, the models based on FFD are truthful only for a limited variety of input process factors. In addition, the progress of higher order FFD models needs a larger number of tests. These attitudes a restriction on the usage of FFD models for non-linear practices, these limitations have resulted in the model progress based on ANNs [14].

Pakravan et al. [15] compared the prognostic and simplification skills of both RSM and ANN employing separate dataset and the correlation coefficients for ANN and RSM were 0.96 and 0.94, respectively. Their studies showed that the modeling ability and results of ANN were superior to RSM.

The RSM conception in the experimental points at three-dimensional spaces can quantitatively and qualitatively reveal the activity relations. This method, in the joint application of RSM and ANN, data that is essential in the ANN can be predicted. Really, by using RSM along with ANN, this problem can be solved [16,17].

The literature review indicates that significant works have been performed on the removal of pCNB [18,19], but based on the author's searches, no paper has been available about using periodate combinations for treatment of pCNB. So, this work was tried to optimize and model the process conditions in the removal of pCNB using a combined statistical method. The researchers can compare the results and found the process better by means of both methods in UV/KPI process [20]. Also, the effects of pH, KPI concentration, and temperature were investigated.

2. Experimental

2.1. Material

pCNB (99.5% purity) was supplied from Merck Company, (Germany) and used without additional purification. Hydrochloric acid (12 M), sodium hydroxide (99%), and potassium periodate (98%) were all provided from Merck Company. Distilled water was used in all tests.

2.2. Photo reactor and experiments

All the experiments were performed in a glass photo reactor with 1 L capacity. The reactor was equipped with sampling system (Fig. 1). A 15 W Philips (UV-C) mercury lamp was inserted vertically in the middle of the reactor as the light source. The set up provided with a jacket of water with an external stream adjusted by a thermostat to adjust the temperature between 25°C and 45°C. The water bath, BW 20G model from Korean Company was employed to control the temperature.

2.3. General procedure

After adding a definite amount of KPI, the solution was transferred to the reactor. The initial pH of the solution was adjusted by H_2SO_4 and NaOH (0.1 N) and measured by pH meter, PT-10P Sartorius Instrument from Germany Company. The progress in the degradation of pCNB was considered by UV/vis spectrophotometer and validated through high pressure liquid chromatography (HPLC). A spectrophotometer (platinum blue) was prepared with HPLC from Knauer, Germany. The length and diameter of the reverse phase column filled with 3 μm Separon C18 were 150 and 4.6 mm, respectively. The isocratic technique was used with a solvent blend of 30% deionized water and 70% methanol through a flow rate at 1 mL/min. About 10 μL of the sample was used for injection and the identification wavelength was 260 nm. The absorbance of chemical oxygen demand (COD) samples was determined at 600 nm by spectrophotometer (DR 5000, Hach, Jenway, USA) [21].

Exactly 1,000 mL of solution containing pCNB was used during each experiment. The reaction at various intervals suggested by the experimental design was started by switching on the UV lamp.

The appropriate efficiencies were calculated with respect to its initial value and the percent of pCNB and COD removal was obtained as the following equations:

$$\text{Removal of pCNB}(\%) = \left(\frac{[\text{pCNB}]_0 - [\text{pCNB}]}{[\text{pCNB}]_0}\right) \times 100 \quad (1)$$

$$\text{Removal of COD}(\%) = \left(\frac{[\text{COD}]_0 - [\text{COD}]}{[\text{COD}]_0}\right) \times 100 \quad (2)$$

where $[\text{pCNB}]_0$ and $[\text{COD}]_0$ are the concentration of the pCNB and amount of COD at the start of the reaction, and [pCNB] and [COD] are their mentioned value at time t, respectively.

The powder of MnO_2 was applied for removing the residual hydrogen peroxide and its interaction with COD test. The samples were filtered to segregate MnO_2 powders [22].

2.4. Optimization procedures and predictive modeling

2.4.1. Artificial neural network

A neural network organization employed in this project is presented in Fig. 2. The ANN construction contains an output layer (dependent variables), hidden layer (hidden), and input layer (independent variables), they are linked by connections with several weights. A joining between output and input layer was provided by hidden layer. In the hidden layer, one or more neurons can be positioned. The ANN with a hidden layer is capable of making the nonlinear equations from existing data.

The topology of an ANN is obtained by the numeral of its layers, nature of transfer functions, and number of nodes in each layer. The most significant stage in the upgrading of the model is optimization of ANN topology. For modeling of pCNB removal, the three layered feed-forward back propagation neural network was used (Fig. 2). In this project, the input variables to the feed-forward neural network include concentration of periodate (mg/L), pH, and temperature (°C). The pCNB removal (%) was selected as output variable or response. The ranges of the used data in ANN are recorded at Table 1.

The various records of neurons, from 5 to 14, in the hidden layer were experienced in this study. Each topology was frequented three times to escape random correlation based on the random initialization of the weights. The correlation between the number of neuron in the hidden layer and the network error are presented in Table 2. The sum of squared error (SSE) and root mean square error (RMSE) were applied as the error function. The efficiency of the network was calculated by RMSE and SSE based on the following equations:

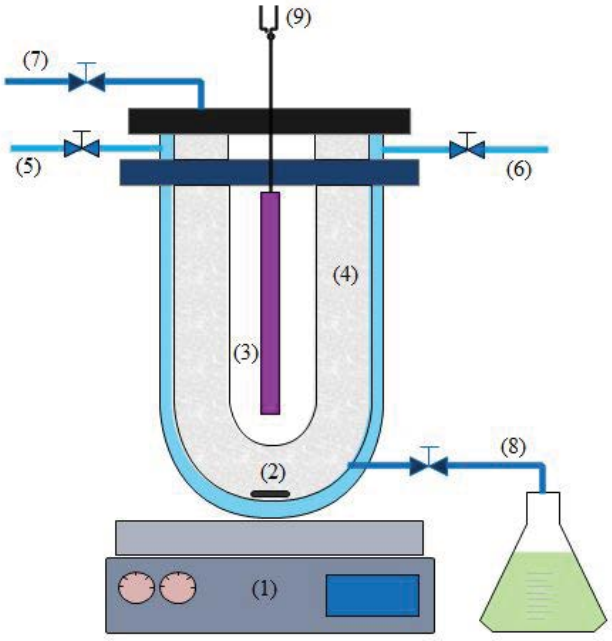

Fig. 1. Graphic plan of the used set up in laboratory scale: (1) magnetic stirrer, (2) magnetic stirrer bar, (3) UV lamp, (4) glass reactor, (5) water supply from thermo bath, (6) water supply to thermo bath, (7) input wastewater, (8) remediated wastewater, and (9) electric construction.

$$\text{RMSE} = \sqrt{\frac{\sum_{i=1}^{i=n}\left(y_{i,\text{pred}} - y_{i,\text{exp}}\right)^2}{N}} \quad (3)$$

$$\text{SSE} = \sum_{i=1}^{i=n}\left(y_{i,\text{pred}} - y_{i,\text{exp}}\right)^2 \quad (4)$$

Moreover, the correlation coefficient is presented in Table 4 which signifies the ratio between the data predicted by the actual data and neural network [15]:

$$R^2 = \frac{\sum_{i=1}^{i=n}\left(y_{i,\text{pred}} - y_{i,\text{exp}}\right)^2}{\sum_{i=1}^{i=n}\left(y_{i,\text{exp}} - y_{i,m}\right)^2} \quad (5)$$

where $y_{i,\text{pred}}$, is the network prediction, n is the numeral of data point, $y_{i,\text{exp}}$ experimental response, y_m average actual,

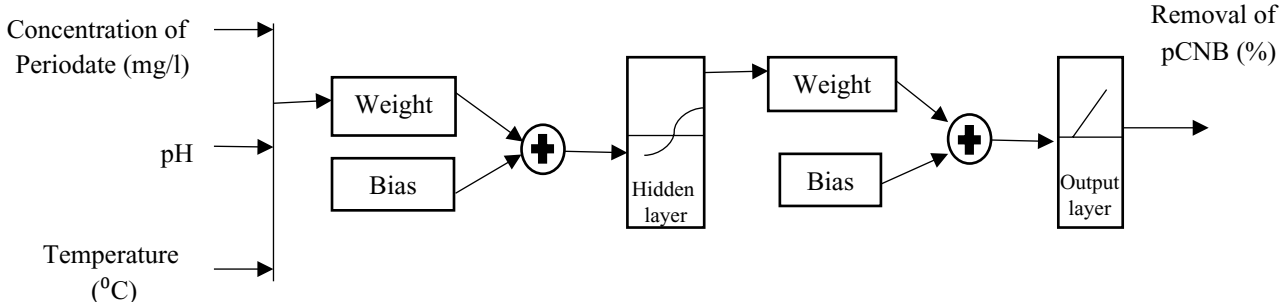

Fig. 2. Structure of ANN for optimization in three layered feed forward back propagation neural network in the modeling of pCNB removal.

Table 1
Variables of model and their used ranges for ANN

Variable	Range
Input layer	
Concentration of periodate (mg/L) (X_1)	150–450
pH (X_2)	4–10
Temperature (°C) (X_3)	25–45
Output layer	
pCNB removal (%)	36.2–97.8

and i is an guide of data. The representation of the network can be strengthened after the presence of adequate number of hidden units just about 16. As it was clear from Table 2, the RMSE and SSE are minimum at 1.0268 and 26.3576, respectively, at about 11 neurons. The R^2 value is in good coincidence with the "R^2_{adj}" values of 0.9973, exhibiting a very good correlation between the actual and predicted data.

The typical ANN is suitable for interpolating data, but it is not good for extrapolating. So, the data designated for training should protect the full variety of input accidental variables to reach a valid ANN model. But, selection of suitable procedures and transfer functions is needed to scheme a correct ANN model; if not, the output outcomes will be defective. Transition function of linear has been employed in output layer and the transition function of Tansig has been applied in the hidden layer. It is superior that targets and inputs are scaled to be in a definite range. Thus, all input data (Y_i) in the range between 0.1 and 0.9 is normalized as the following (Y_{norm}) equation:

$$Y_{norm} = 0.8\left(\frac{Y_i - Y_{i,min}}{Y_{i,max} - Y_{i,min}}\right) + 0.1 \quad (6)$$

where the extreme values of Y_i are $Y_{i,min}$ and $Y_{i.max}$ [23]. All output returned to its original scale after the training of the network, and then the experimental design was compared to response predicted by the experimental results.

Table 2
Effect of the number of neurons in the hidden layer on the function of the neural network

N	R^2	R^2_{adj}	RMSE	SSE
5	0.9924	0.9921	1.6897	71.3761
6	0.9784	0.9775	2.7962	195.4685
7	0.9063	0.9026	5.5456	768.8438
8	0.8805	0.8757	7.8664	1,547
9	0.9311	0.9284	5.3319	710.7329
10	0.9875	0.9870	2.1547	116.0671
11	0.9974	0.9973	1.0268	26.3576
12	0.8836	0.8790	7.9070	1,563
13	0.8625	0.8612	7.9557	1,637
14	0.9101	0.9065	6.3220	999.1822
15	0.8759	0.8709	7.4352	1,382.1

The correlation coefficient (R) identifies the degree of connotation between variables. A correlation value of 0 is supposed to be the lack of linear correlation, though 1 suggests perfect correlation between variables. The R^2 value inside the range of 0.7–1.0 implies a suitable result. The persistent repetition of weight variables was done to obtain a model with the best possible fit. The best solution as found at the 11th iteration with the minimum MSE value and the maximum R-values for training, validation, and testing. The solution of the programmed ANN method is gained at the 11th row with lowest MSE value.

2.4.2. Full factorial design method

The FFD was used with three independent parameters including the concentration of periodate (mg/L) (X_1), pH, and temperature (°C). The pCNB removal percentage was selected as response and the experimental design was employed to obtain the optimum conditions. According to the previous studies and initial tests, the ranges of variables for FFD were chosen. The input parameters and their levels in the test are presented in Table 3.

The FFD is a complete DOE that all levels of each variable in an experiment are joined with all levels of other variable.

In this study, 27 tests were run distinctly. For reducing experimental errors, all factorial designs were performed randomly. The F-test analysis of variance with a 95% confidence interval was used to consider the statistical influence of the important variables and their connections.

The resulting model in the form of a polynomial equation was fitted to the response variable (Y) (Eq. 7):

$$Y = b_0 + \sum b_i x_i + \sum\sum b_{ij} x_i x_j + \sum\sum b_{ii} x_i^2 + \varepsilon \quad (7)$$

where the residual term is ε, b_0 is a constant, b_{ij} is the linear interaction influence between the input variables, x_i and x_j (i = 1, 2, and 3; j = 1, 2, and 3) are independent variables, the slope of variable is b_i, b_{ii} is the second order of input variable (x_i). The ANOVA was used to investigate the importance of each term in the polynomial equation [24]. The MINITAB 17 was used to get the coefficients of Eq. (3) by FFD. The experimental design includes 27 runs and the ordinary values of these variables, the predicted, and experimental response values for the removal of pCNB are presented in Table 4. In all runs, the concentration of pCNB was 50 mg/L and the time of reaction was 90 min.

3. Results and discussion

3.1. FFD analysis

The purpose of this part was to state the best condition for highest removal of pCNB. The FFD was used to get the important effect of the key factors and their interactions on the removal of pCNB (%). The F-ratio, P-value, sum of squares, and mean square of each variable, are presented in Table 5. The significance of the data was judged by its P-value and the values closer to zero meaning more importance. The P-value should be equal to or less than 0.05 to study statistically important for 95% confidence level. Many researchers studied the steps of the FFD [25,26].

Table 3
Range and levels of variables in FFD design and ANN input variables

Variables	Range and levels		
	Level 1 (–1)	Level 2 (0)	Level 3 (+1)
Concentration of periodate (KPI) (mg/L) (X_1)	150	300	450
pH (X_2)	4	7	10
Temperature (°C) (T) (X_3)	25	35	45

Table 4
FFD and ANN in the removal of pCNB (%) by UV/KPI process at 90 min of reaction

Number	Concentration of periodate (mg/L)	pH	Temperature (°C)	pCNB removal % (Exp)	ANN = 11	FFD
1	300	7	25	90.0	89.71	89.93
2	150	7	35	56.5	56.5	53.82
3	150	7	45	53.0	52.58	53.95
4	300	7	45	94.0	94.96	97.17
5	300	4	25	79.2	80.42	79.76
6	450	7	35	93.0	92.99	94.28
7	300	7	35	97.8	97.79	99.02
8	300	10	35	87.5	87.5	82.83
9	450	10	45	77.9	77.9	75.96
10	450	7	25	88.0	87.99	87.47
11	300	10	25	76.5	79.25	74.67
12	150	10	25	36.2	36.20	38.96
13	450	7	45	91.5	92.55	90.80
14	150	7	25	50.3	50.3	49.19
15	150	10	35	45.5	45.50	43.61
16	450	4	35	79.0	79.00	82.38
17	300	10	45	79.8	79.79	79.91
18	150	4	35	49.0	48.99	48.92
19	450	4	45	80.0	79.79	79.52
20	300	4	45	88.5	88.49	87.01
21	150	10	45	44.2	44.20	43.51
22	150	4	25	40.5	36.20	43.28
23	450	10	35	79.0	78.30	79.45
24	150	4	45	48.0	48.00	49.27
25	300	4	35	93.3	93.29	88.25
26	450	4	25	77.0	76.99	76.07
27	450	10	25	74.4	74.40	74.07

3.1.1. ANOVA tests for the removal of pCNB in UV/KPI process

In this project, the influence of three independent factors on the response was explored by using FFD, to get the optimum conditions. The mathematical relationship between the response and three significant variables can be calculated by a quadratic polynomial equation [27]. An empirical relation between the response (removal of pCNB) and independent variables was achieved and expressed by the following second-order polynomial equation:

$$\text{Removal of pCNB}(\%) = 1.035 + 0.1084X_{C_{KPI}} + 0.2178X_{C_{PH}} + 0.0496X_{C_T} - 0.000015X_{C_{KPI}}^2 - 0.017X_{C_{PH}}^2 - 0.00057X_{C_T}^2 + 0.000044X_{C_{KPI}}X_{C_{PH}} - 0.000014X_{C_{KPI}}X_{C_T} - 0.00016X_{C_{PH}}X_{C_T} \quad (8)$$

The statistical features of designated important model terms are presented in Table 5 for introduction of the pCNB removal efficiency.

For offered model, a list of data such as the ANOVA and coefficients is presented in Table 5 for testing the

Table 5
ANOVA tests for quadratic models in the removal of pCNB by UV/KPI process

Source	DF	Adj. SS	Adj. MS	*F*-value	*P*-value
Model	18	9,567.58	531.53	112.82	0.000
Linear	6	9,484.37	1,580.73	335.51	0.000
[KPI] (mg/L)	2	8,417.18	4,208.59	893.26	0.000
pH	2	853.73	426.77	90.60	0.000
T (°C)	2	213.46	106.73	22.65	0.001
Two way interaction	12	83.21	6.93	1.47	0.298
[KPI] × pH	4	53.03	13.26	2.81	0.099
[KPI] × *T* (°C)	4	17.44	4.36	0.93	0.495
pH × *T* (°C)	4	12.74	3.18	0.68	0.627
Error	8	37.69	4.71		-
Total	26	9,605.27			-
Model summary	*S*	R^2	R^2_{adj}	R^2_{pred}	
	1.20880	98.86	98.72	95.53	

importance of the regression coefficient. It is clear that, more than 95% of the data (R^2 = 98.86%, adjusted R^2 = 98.72%) can be forecasted by the model, suggesting that the terms which were resented in the proposed model are noteworthy to make acceptable predictions. However, the addition of more terms raises the predictions of the model. The R^2 value was close to unit for this model, which suggests that the model is acceptable. The *F*-value of model is valued as the ratio of mean square residual and mean square regression. Actually, the high value of *F*-ratio (112.82) approves the importance of the suggested model.

The *P*-value of model is very small (0.000), which signifies the importance of the model [18].

3.1.2. Main and interaction effect plots

The main effect (mean) plot is suitable for investigation of the data in a designed experiment with respect to main variables which were at two or more levels. In the removal of pCNB, the main effect plots of three variables are presented in Fig. 3. As revealed, the pH has an important effect on the response.

3.2. Prognostic modeling with ANN

The displayed DOE in Table 4, is employed for training the network and experimental pCNB removal. The ANN was applied by using the most common feed-forward construction, that is, multi-layer perceptron (MLP) with logistic sigmoidal function. The MLP network has three input nodes on behalf of independent factors and one output node representing the pCNB removal (%). The training cycle was performed for changing numbers of neurons in the hidden layer and similarly for different blends of ANN-specific parameter such as random initialization and learning rate. Fig. 4 shows an evaluation between experimental values and calculated of the output variable for data set by using FFD and neural network model with the correlation coefficient of 0.9886 and 0.9974, respectively, and states the reliability and very good fit of the model.

These results were presented a good agreement between actual and predicted values. The predicted response from the model is in agreement with the experimental data.

From Fig. 4, it can be seen that the achieved results from the suggested ANN and ANOVA model are in good covenant with the trial data. The simplification and prognostic abilities of both FFD and ANN were compared. The ANN model was a little better than FFD model with lower RMSE (1.0268AAN < 2.055838 FFD).

3.3. ANN modeling

For modeling the system, the tests were designed according to the FFD and ANN. The concentrations of Periodate, temperature, and pH were selected as independent variables and the efficiency of pCNB removal was chosen as the response. It was discovered that the predictive capacity of ANN model is more than FFD because of their corresponding R^2, R^2_{adj}, RSME, and SSE.

In this study, a three-layered backpropagation ANN was selected containing an input layer (independent factors), an output layer (dependent variable), and a hidden layer. A tangent sigmoid (tansig) transfer function was used to activate the hidden layer, while a linear (purelin) function for the input/output layers. For training aims the Levenberg–Marquardt back propagation algorithm was selected [28,29]. In this study, the neural network toolbox of Matlab 2017 (MATLAB R2016b) mathematical software was used for the prediction of pCNB degradation. A critical factor for the progress of an ANN is the topology (optimum number of neurons). As can be seen from Fig. 5, about 70% of the data was used for network training and 15% for data validation and testing [30].

The scatter charts that match the actual data against the calculated neural network data in training, validation, and testing networks are illustrated in Fig. 5. Nearly all data scatter nearby the 45° line that is the sign of exceptional compatibility between ANN predicted data and experimental results. It is obvious that the trained neural network has competent estimated experimental values. According

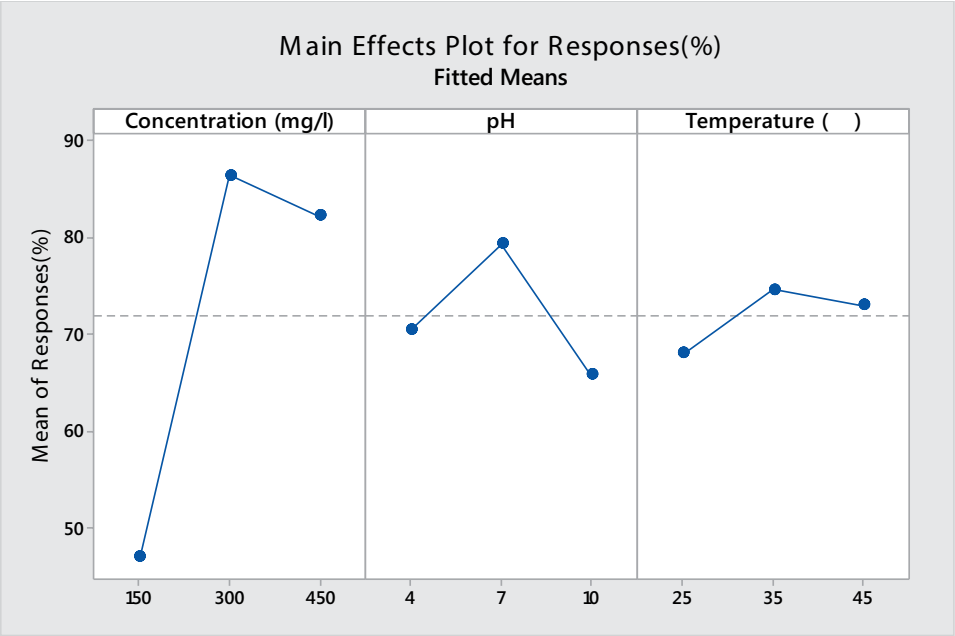

Fig. 3. Main effect plots for pCNB removal (%) in uncoded values at 90 min.

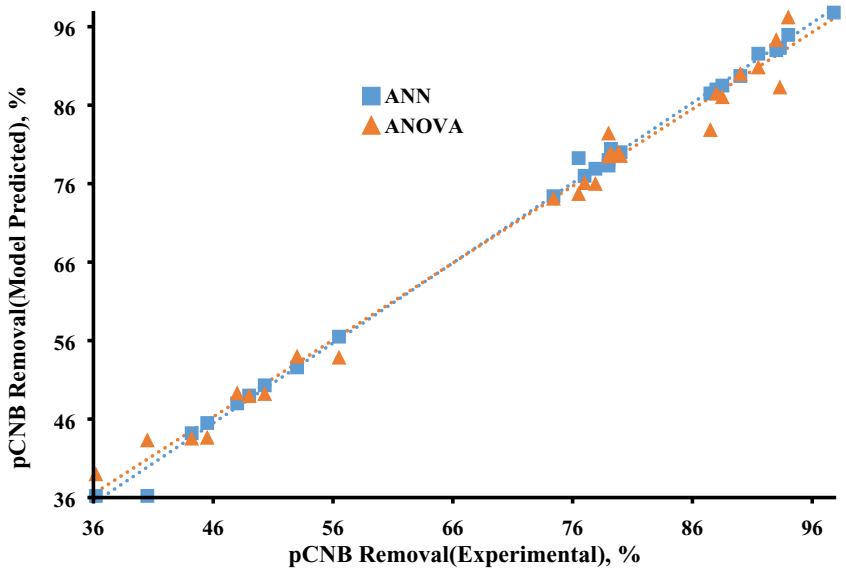

Fig. 4. Comparing the experimental and predicted ANN and ANOVA values for the removal of pCNB in UV/KPI process.

to Fig. 5, the straight lines are the linear relations between the target and output data used in this project. The correlation coefficients (R) among the predicted and experimental values are 0.99898 (training), 0.999 (testing), and 1.0 (validation). Thus, the ANN prediction for training, testing, and validation is highly significant and commendable in terms of correlation.

3.4. Influence of operative variables

According to the model (Eq. (8)), two-dimensional contour plots for the measured response were designed to achieve a superior consideration in the interaction properties of variables in the removal efficiency of pCNB.

The effects of operational variables are displayed by contour plots, where the influence of two variables are measured but the third is fixed. The influences of the concentration of KPI and initial pH on the degradation of the pCNB are shown in Fig. 6a.

The pCNB removal efficiency reaches a great value at pH of 7.0 and reduces at both higher and lower pH values. The production of hydroxyl radicals is catalyzed by protonation of $O^{\bullet -}$ radicals, at slight acidic conditions, and in turn, hydroxyl radicals are produced. The falling trend in the

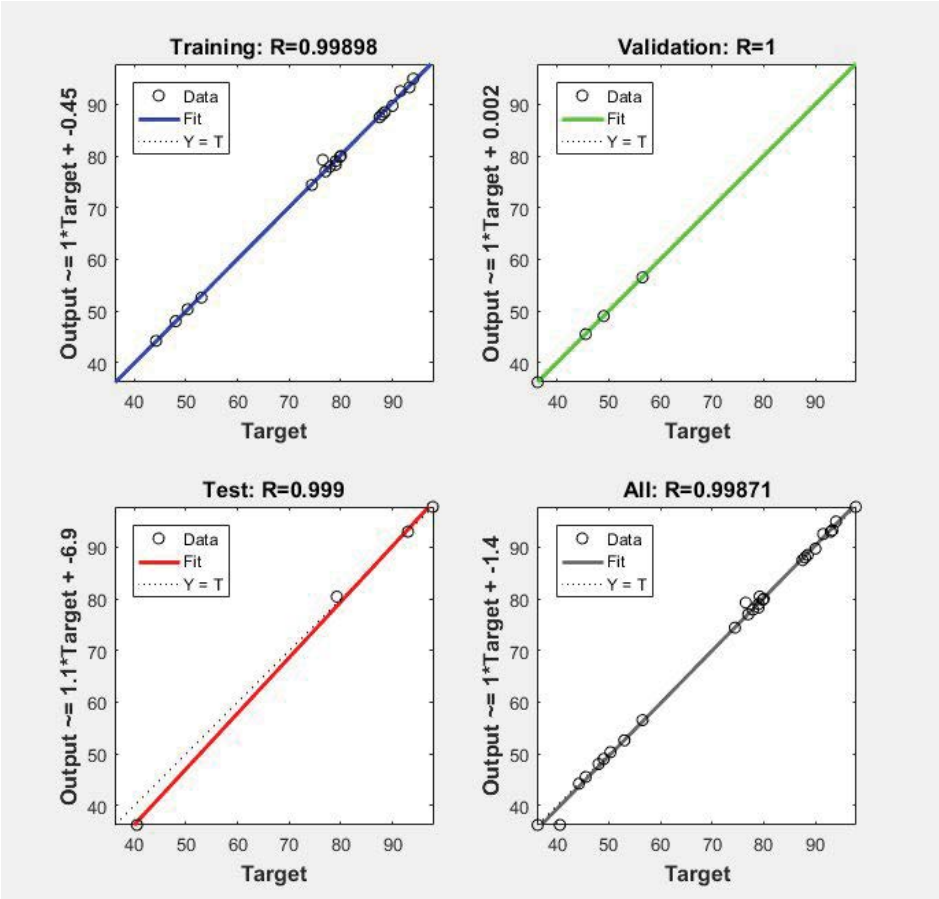

Fig. 5. Evaluation between the experimental values of pCNB removal and predicted values by ANN for training, testing, and validation and all prediction set.

pCNB removal at strong acidic pH could be originated from the scavenging effect of hydroxyl radicals by the high dosage of chloride ions, incoming to the solution by HCl, which was added for pH regulation, and changing the radicals to the fewer active oxidants such as $Cl_2^{\bullet-}$ based on the resulting reactions [31]:

$$Cl^- + OH^\bullet \rightarrow ClOH^{\bullet-} \quad (9)$$

$$ClOH^{\bullet-} + H^+ \rightarrow H_2O + Cl^\bullet \quad (10)$$

$$Cl^- + Cl^\bullet \rightarrow Cl_2^{\bullet-} \quad (11)$$

The state of pCNB in molecular or ionic species will change at different pH. It was obvious from Fig. 6a, that the highest degradation of pCNB was gained in the pH range of 7, which is approximately around the pKa of the pCNB, which is 7.1. Therefore, the pCNB can be in molecular or anionic construction at high and low pH values, respectively. So, the removal of pCNB is decreased at alkaline pH values because of the electrostatic repulsion between anionic pCNB and IO_4^- ions.

Also, Fig. 6b, displays that by increasing the concentration of KPI, the removal of pCNB rises, which is originated from the manufacture of $IO_4^\bullet$, $IO_3^\bullet$, and $OH^\bullet$ radicals. It should be noted that the addition of KPI in excess amounts, could cause less removal in pCNB because of periodate dimerization:

$$2IO_4^\bullet \rightarrow I_2O_8 \quad (12)$$

In addition, reduction in pCNB removal with combining IO_4^- ions can be originated from the scavenging of hydroxyl radicals with this ion as the following equation [32]:

$$IO_4^- + OH^\bullet \rightarrow IO_4^\bullet + OH^- \quad (13)$$

As it is clear from Fig. 6c, the pCNB removal was increased with increase in temperature, but further rise in temperature after certain values, had no significant effect on the removal of pCNB. At high temperatures (45°C), the periodate radicals can combine and create inactive agents and then the advancement of reaction decreased [33].

The operational variables were optimized to get the maximum removal of pCNB at 97.8% after 90 min the optimum removal of pCNB was predicted at 99.02% in optimum conditions; [KPI] = 300 mg/L, pH = 7.0, and T = 35°C.

The removal percent of COD in the treatment of pCNB by UV/KPI process at optimum conditions was 64.3% after 90 min. It should be noted that the degradation of pCNB

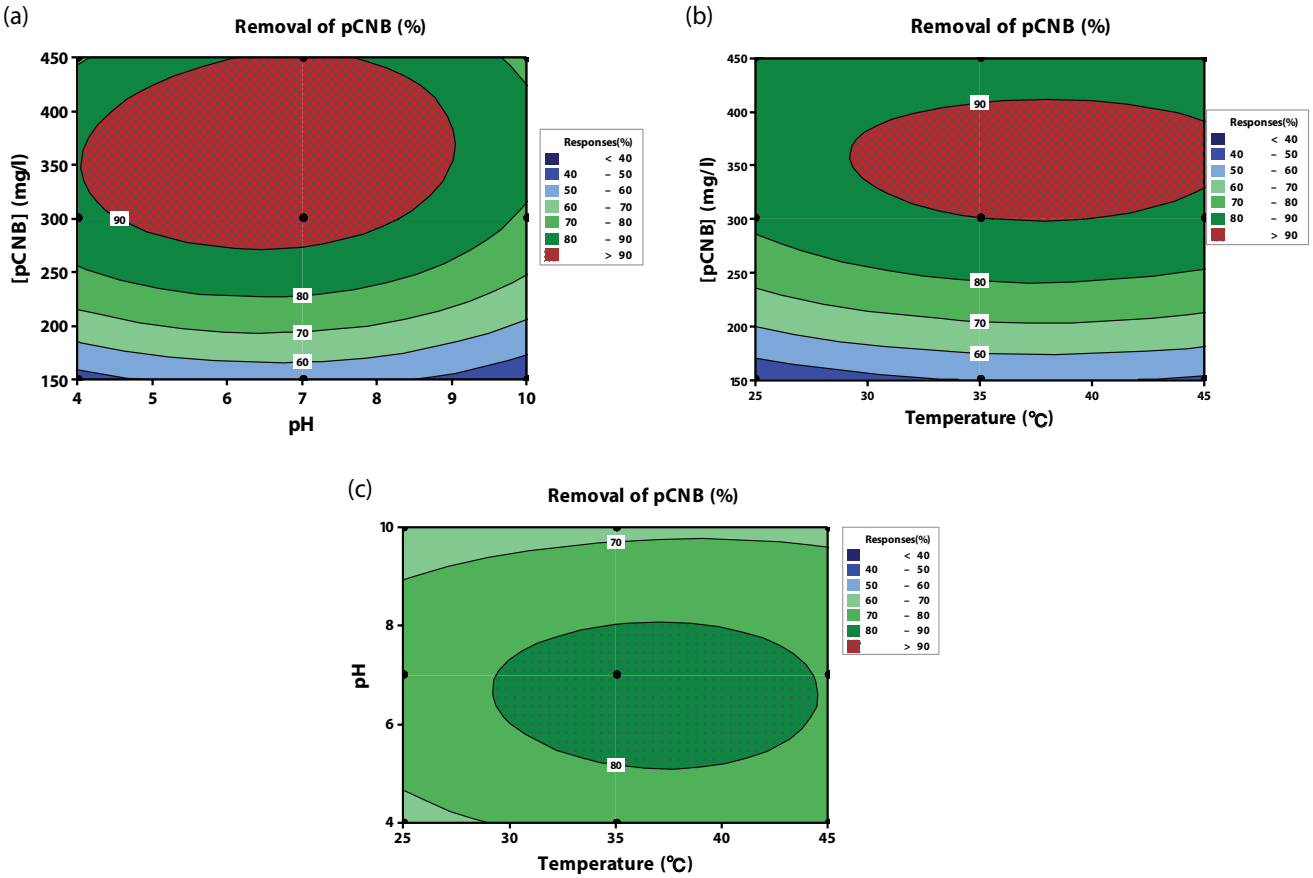

Fig. 6. Contour (2D) plots for the removal of pCNB vs. independent variables ((a) pH and concentration of periodate, (b) concentration of periodate and temperature, and (c) pH and temperature).

Table 6
Comparison of predictive capability of FFD and ANN

Parameters	ANN	FFD
RMSE	1.0268	2.0558
SSE	26.3576	114.1147
R^2	0.9974	0.9886
R^2_{adj}	0.9973	0.9872
Average % error	0.4328	1.5706

using single UV irradiation was only 7.6% after 90 min, and about 3% of degradation has happened while using only KPI reagent without UV light in the darkness.

3.5. Comparison between factorial design and ANNs

Fig. 4 displays an assessment between the calculated degradation of pCNB values and those predicted by the factorial design and ANN methods for typical runs. As it can be seen from Table 6, the ANN simulates the process better, from a mathematical viewpoint in terms of R^2 and RMSE, which is because of its non-linear performance within the range of the operational investigated factors. Meanwhile, the FFD has many benefits such as a simple explanation of the outcomes and the probable relationship with the physical meaning of the considered system, and acceptable outcomes can be obtained using a very low number of tests and calculations, therefore saving costs and time. However, ANN is typically considered as black box in the literature [15], but the analysis gives precisely the same order of the important factors for both ANN and FFD. Also, this is correct when the results of FFD design method are re-analyzed ignoring all interactions (simple first-order analysis). This shows that ANN can also be used to get some valuable facts about the properties of the system and not only as a method for simulation and prediction of data.

4. Conclusions

In this research, the FFD and ANN were used to investigate the effects of experimental parameters including temperature, initial KPI concentration, and pH on the degradation of pCNB by UV/periodate process. The effect of the main process variables on pCNB removal was investigated. The optimal conditions were obtained as 300 mg/L of KPI, pH of 7.0, and temperature at 35°C. The removal of the pCNB at optimum condition was 97.8%, and the predicted values by ANN and FFD methods were 97.79% and

99.02%, respectively. At these conditions about 64.3% of COD was removed after 90 min of reaction.

The most significant features in this project are as the following: (i) high degradation efficiency was obtained in mild optimum conditions, (ii) the investigation of scavenging effect showed that all active radicals particularly hydroxyl radical have a main role in degradation of pCNB, and (iii). The ANN has better performance than FFD for the simulation of the process, although it requires considerably larger sets of data and computational time.

For ANN and FFD, the correlation coefficients were 0.9974% and 0.9886%, respectively. The ability of ANN modeling has presented its supremacy over FFD with relative fewer values of average percentage error and RMSE.

Acknowledgments

The authors wish to acknowledge the HSE section of national petrochemical company of Iran for technical leadership.

References

[1] T. Oki, S. Kanae, Global hydrological cycles and world water resources, Science, 313 (2006) 1068–1072.
[2] M. Mohadesi, A. Shokri, Evaluation of Fenton and photo-Fenton processes for treatment of aqueous environment containing p-chloronitrobenzene, Desal. Water Treat., 81 (2017) 199–208.
[3] A. Shokri, the treatment of spent caustic in the wastewater of olefin units by ozonation followed by electrocoagulation process, Desal. Water Treat., 111 (2018) 173–182.
[4] A. Shokri, Degradation of 4-nitrophenol from industrial wastewater by nano catalytic ozonation, Int. J. Nano Dimens., 7 (2016) 160–167.
[5] A. Shokri, A.H. Joshaghani, Using microwave along with TiO_2 for the degradation of 4-chloro-2-nitro phenol in aqueous environment, Russ. J. Appl. Chem., 89 (2016) 1985–1990.
[6] W. Choy, W. Chu, Photo-oxidation of o-chloroaniline in the presence of TiO_2 and IO_3^-: a study of photo-intermediates and successive IO_3^- dose, Chem. Eng. J., 136 (2008) 180–187.
[7] C. Lee, J. Yoon, Application of photo activated periodate to the decolorization of reactive dye: reaction parameters and mechanism, J. Photochem. Photobiol., A, 165 (2004) 35–41.
[8] W.A. Sadik, Effect of inorganic oxidants in photodecolourization of an azo dye, J. Photochem. Photobiol., A, 191 (2007) 132–137.
[9] J. Saien, M. Fallah Vahed Bazkiaei, Homogenous UV/periodate process in treatment of p-nitrophenol aqueous solutions under mild operating conditions, Environ. Technol., 39 (2018) 1823–1832.
[10] Z. Kim, Y. Shin, J. Yu, G. Kim, S. Hwang, Development of NO_x removal process for LNG evaporation system: comparative assessment between response surface methodology (RSM) and artificial neural network (ANN), J. Ind. Eng. Chem., 74 (2019) 136–147.
[11] M.R. Gadekar, M.M. Ahammed, Modelling dye removal by adsorption onto water treatment residuals using combined response surface methodology-artificial neural network approach, J. Environ. Manage., 231 (2019) 241–248.
[12] A.M. Ghaedi, S. Karamipour, A. Vafaei, M.M. Baneshi, V. Kiarostami, Optimization and modeling of simultaneous ultrasound-assisted adsorption of ternary dyes using copper oxide nanoparticles immobilized on activated carbon using response surface methodology and artificial neural network, Ultrason. Sonochem., 51 (2019) 264–280.
[13] F.M. Elfghi, A hybrid statistical approach for modeling and optimization of RON: a comparative study and combined application of response surface methodology (RSM) and artificial neural network (ANN) based on design of experiment (DOE), Chem. Eng. Res. Des., 113 (2016) 264–272.
[14] S. Ghanavati Nasab, A. Semnani, A. Teimouri, M. Javaheran Yazd, T. Momeni Isfahani, S. Habibollahi, Decolorization of crystal violet from aqueous solutions by a novel adsorbent chitosan/nanodiopside using response surface methodology and artificial neural network-genetic algorithm, Int. J. Biol. Macromol., 124 (2019) 429–443.
[15] P. Pakravan, A. Akhbari, H. Moradi, A. Hemati Azandaryani, A.M. Mansouri, M. Safari, Process modeling and evaluation of petroleum refinery wastewater treatment through response surface methodology and artificial neural network in a photocatalytic reactor using pol ethyleneimine (PEI)/titania (TiO_2) multilayer film on quartz tube, Appl. Petrochem. Res., 5 (2015) 47–59.
[16] A. Shokri, Degradation of 4-chloro phenol in aqueous media thru UV/persulfate method by artificial neural network and full factorial design method, Int. J. Environ. Anal. Chem., 1 (2020) 1–15.
[17] S.N.A. Sanusi, M.I.E. Halmi, S.R.S. Abdullah, H.A. Hassan, F.M. Hamzah, M. Idrisc, Comparative process optimization of pilot-scale total petroleum hydrocarbon (TPH) degradation by *Paspalum scrobiculatum* L. Hackusing response surface methodology (RSM) and artificial neural networks (ANNs), Ecol. Eng., 97 (2016) 524–534.
[18] H. Li, L. Zhou, H. Lin, X. Xu, R. Jia, S. Xia, Dynamic response of biofilm microbial ecology to para-chloronitrobenzene biodegradation in a hydrogen-based, denitrifying and sulfate-reducing membrane biofilm reactor, Sci. Total Environ., 643 (2018) 842–849.
[19] R. Ma, J. Shen, A. Li, Aqueous meta-chloronitrobenzene degradation by ozonation and its kinetics, Ozone Sci. Eng., 36 (2014) 496–501.
[20] J. Prakash Maren, B. Priya, Comparison of response surface methodology and artificial neural network approach towards efficient ultrasound-assisted biodiesel production from muskmelon oil, Ultrason. Sonochem., 23 (2015) 192–200.
[21] American Public Health Association, American Water Works Association, Water Pollution Control Federation, and Water Environment Federation, Standard Methods for the Examination of Water and Wastewater, Vol. 2, American Public Health Association, 1915.
[22] M. Mohadesi, A. Shokri, Treatment of oil refinery wastewater by photo-Fenton process using Box–Behnken design method: kinetic study and energy consumption, Int. J. Environ. Sci. Technol., 16 (2018) 7349–7356.
[23] M. Zarei, A. Niaei, D. Salari, A.R. Khataee, Removal of four dyes from aqueous medium by the peroxi-coagulation method using carbon nanotube–PTFE cathode and neural network modeling, J. Electroanal. Chem., 639 (2010) 167–174.
[24] H. Moradi, S. Sharifnia, F. Rahimpour, Photo catalytic decolorization of reactive yellow 84 from aqueous solutions using ZnO nanoparticles supported on mineral LECA, Mater. Chem. Phys., 158 (2015) 38–44.
[25] S. Alizadeh Kordkandi, M. Forouzesh, Application of full factorial design for methylene blue dye removal using heat-activated persulfate oxidation, J. Taiwan Inst. Chem. Eng., 45 (2014) 2597–2604.
[26] A. Shokri, Application of Sono–photo-Fenton process for degradation of phenol derivatives in petrochemical wastewater using full factorial design of experiment, Int. J. Ind. Chem., 9 (2018) 295–303.
[27] A. Shokri, Investigation of UV/H_2O_2 process for removal of Ortho-Toluidine from industrial wastewater by response surface methodology based on the central composite design, Desal. Water Treat., 58 (2017) 258–266.
[28] Z. Frontistis, C. Drosou, K. Tyrovola, D. Mantzavinos, D. Fatta-Kassinos, D. Venieri, N.P. Xekoukoulotakis, Experimental and modeling studies of the degradation of estrogen hormones in aqueous TiO_2 suspensions under simulated solar radiation, Ind. Eng. Chem. Res., 51 (2012) 16552–16563.
[29] A.R. Khataee, M.B. Kasiri, Artificial neural networks modeling of contaminated water treatment processes by homogeneous and heterogeneous nano catalysis, J. Mol. Catal. A: Chem., 331 (2010) 86–100.

[30] C.A. Igwegbe, L. Mohmmadi., S. Ahmadi, A. Rahdar, D. Khadkhodaiy., R. Dehghani, S. Rahdar, Modeling of adsorption of Methylene Blue dye on Ho-$CaWO_4$ nanoparticles using response surface methodology (RSM) and artificial neural network (ANN) techniques, MethodsX, 6 (2019) 1779–1797.
[31] G. Le Truong, J. De Laat, B. Legube, Effects of chloride and sulfate on the rate of oxidation of ferrous ion by H_2O_2, Water Res., 38 (2004) 238423–238494.
[32] C.G. Silva, J.L. Faria, Photochemical and photocatalytic degradation of an azo dye in aqueous solution by UV irradiation, J. Photochem. Photobiol., A, 155 (2003) 133–143.
[33] J. Sirvio, U. Hyvakko, H. Liimatainen, J. Niinimaki, O. Hormi, Periodate oxidation of cellulose at elevated temperatures using metal salts as cellulose activators, Carbohydr. Polym., 83 (2011) 1293–1297.